

Calibration of large water-Cherenkov Detector at the Sierra Negra site of LAGO

A. Galindo^a

E-mail: alinegalindo@inaoep.mx

E. Moreno^b

E-mail: eduardo.moreno.barbosa@cern.ch

E. Carrasco^a

E-mail: bec@inaoep.mx

I. Torres^a

E-mail: ibrahim@inaoep.mx

A. Carramiñana^{a*}

E-mail: alberto@inaoep.mx

For the LAGO Collaboration,

see the full list of members and institutions at <http://lagoproject.org/colab.html>

^a *Instituto Nacional de Astrofísica, Óptica y Electrónica*

^b *Benemérita Universidad Autónoma de Puebla*

The Latin American Giant Observatory (LAGO) is an international network of water-Cherenkov detectors (WCD) set in different sites across Latin America. On the top of the Sierra Negra volcano at 4530 m a.s.l., LAGO has completed its first instrumented detector of an array, consisting of a cylindrical WCD with 7.3 m in diameter and 1 m of height, with a total detection area of 40 m² and sectioned in four equal slices. Each one of these slices is instrumented with an 8" photo-multiplier tube installed at the top of the detector and looking downwards. The final setup will have three WCD as the one mentioned, distributed in triangular shape and one WCD with 7.3 m in diameter and 5 m of height located in the centre. The data acquisition of this first WCD started in June 2014. In this work the full calibration procedure of this detector will be discussed and the preliminary measurements of stability in rate.

*The 34th International Cosmic Ray Conference,
30 July- 6 August, 2015
The Hague, The Netherlands*

*Speaker.

1. Introduction

The Earth is constantly bombarded by particles, cosmic rays and photons, originated in outer space. These particles can be effectively detected in indirect mode on the Earth's surface by collecting the secondary particles generated from the interaction of primary particles at the top of the atmosphere. The collisions give rise to Extensive Air Showers (EAS), integrated by hadronic, electromagnetic, muon and neutrino components. If the primary is a photon, the electromagnetic component is dominant. The electromagnetic and muon components are identified with ground detectors, the hadronic component dies away soon after the primary collision transforming into other components and neutrinos do not interact enough to be detected.

Water Cherenkov detectors (WCD) are successfully used to detect secondary particles. They travel at relativistic velocities, leaving behind Cherenkov light easily detectable by photomultiplier tubes (PMT). The Latin American Giant Observatory uses WCD in order to detect gamma ray bursts (GRBs) using the single particle technique, which looks for increases in the background rate on all detectors in a short period of time due to the arrival of many photons during a burst [1]. LAGO detectors are also used to study the solar activity and space weather.

We describe the calibration of the detector, including the PMTs characterization. We present preliminary data of the stability of the rate over time.

2. Experimental setup

LAGO is located at the top of the Sierra Negra volcano at 4530 m a.s.l. It consists of three cylindrical aluminum WDCs situated each in a corner of a triangle array, with 1.2 m of height and 7.3 m in diameter. The detectors are divided in fourth by walls and a PMT of 8 " model 9354KBL is placed at 2 m of distance from the detector's center in the central axis of every fourth. The inner surfaces and the walls are covered by a high diffusive and reflective Tivek[®] material, the detectors are filled up at 1 m with purified water. An additional WDC with same diameter but 5.0 m in height will be installed at the barycenter of the array.

3. Calibration

3.1 Calibration of PMTs

Each PMT was tested against the specifications given by ET Enterprises, to ensure that only PMTs of desired quality are used in the detector. The measurement of the single photoelectron spectrum (SPE) was required in order to determinate the absolute gain of the PMT [2]. This is done by flashing a LED at an intensity such that there is a ratio of 1/10 of signal-noise relation present on the photocathode. A schematic of the SPE setup is shown in figure 1. The acquisition system was conformed by CAEN devices based on VME bus, such as crate VME mod. 8011, a digitizer card mod. V1751, HV supply mod. V6533 and a USB bridge mod. V1718.

To determine a suitable intensity for the light source to achieve the desired ratio, an offline calibration was performed. The light intensity was varied by changing the width of a pulsed signal with 800 mVpp, 1.2 V offset and frequency of 1 KHz. When it was observed one pulsed signal from the PMT per 10 noise signals, the intensity of the light source was fixed, this ensures that any

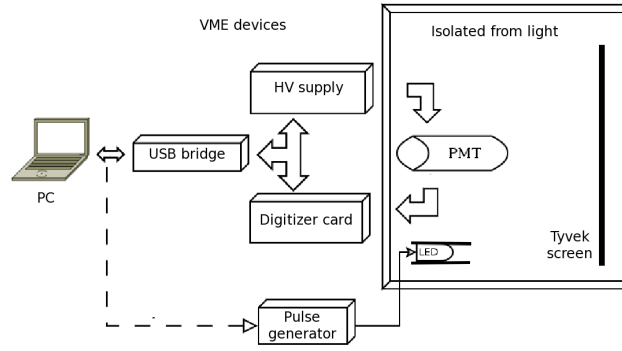


Figure 1: Schematic of the SPE setup.

signal observed above the noise is predominantly from SPEs [3]. The voltage supply for the PMT was set at the nominal value given by the manufacturer. The traces taken were processed to obtain charges distributions. A typical SPE distribution can be seen in figure 2.

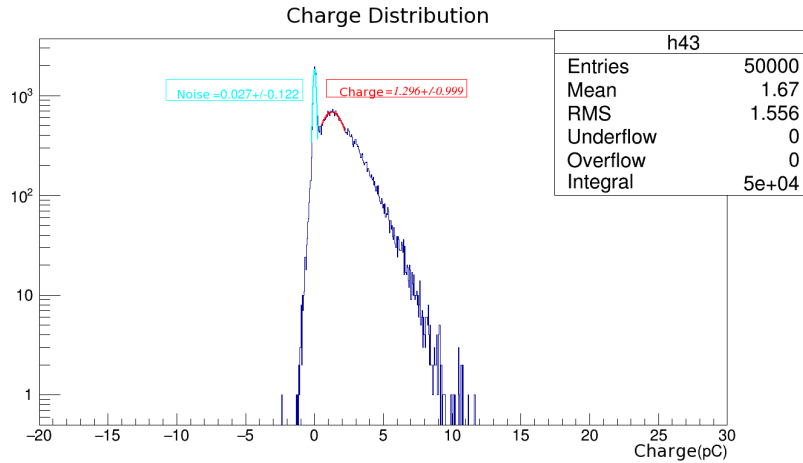


Figure 2: Typical single photoelectron distribution. The first peak is the noise and the second peak is due to 1 pe event, taken from the PMT with serial number 7089, feeded with 1500 Volts, 50000 traces.

To calculate the gain it was necessary to find the mean and the deviation of the photoelectron signal directly from the measured. The charge fit was divided by the known value of 1 pe charge, 1.602×10^{-19} C [4]. Once the gain is calculated, the absolute gain at that voltage is known. However, it was necessary to have several points to determine the gain as a function of the input voltage, so we obtained distributions with different values of voltage supply. The results of this test for the PMTs working in the site are shown in the figure 3. Now, we have a reference to set a voltage supply for each one in order to have similar gain value in all the PMTs, or at least to have in account the proportionality of gain in the data process.

3.2 WCD calibration

A typical way to calibrate WCDs is done by measuring the natural flux of secondary particles through the detector. Nevertheless, calibrating and monitoring a WCD at high altitude is not easy.

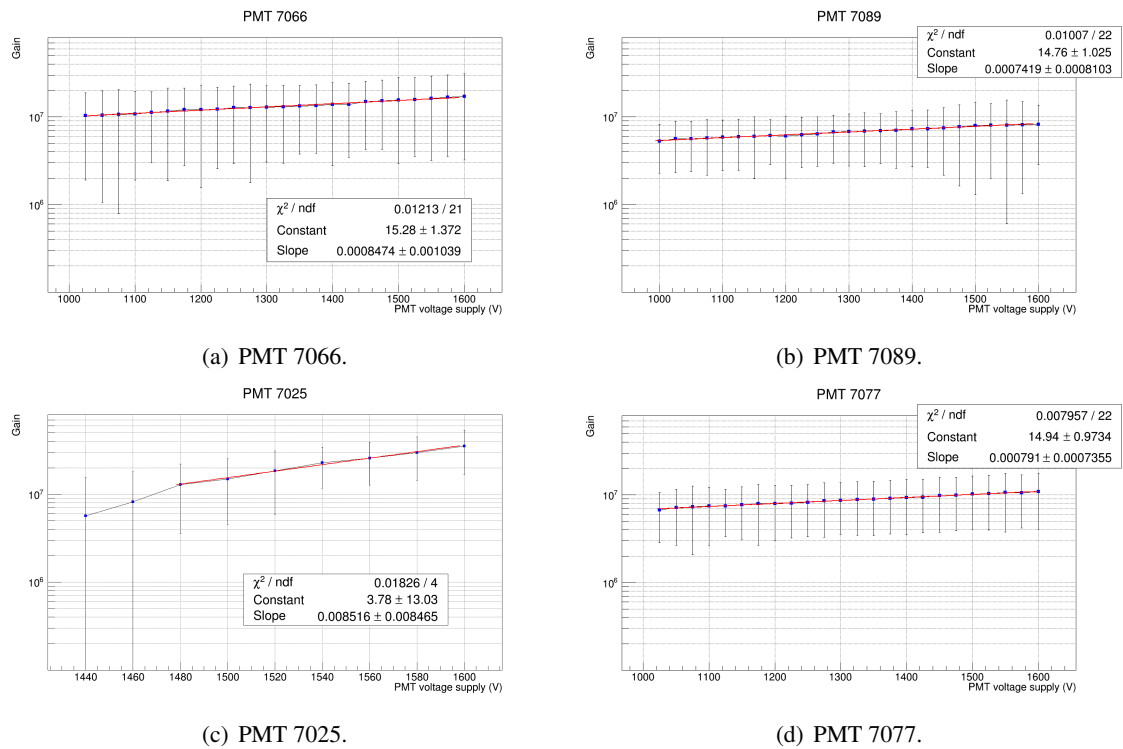


Figure 3: Curves for the gain as a voltage function for the PMTs tested.

At low altitudes, background muons provides a natural mark easy to detect and calibrate [5], but at high altitude the electromagnetic component dominates over the mounic component.

At Sierra Negra, we need to use the muon peak as a calibration mode. We implemented a data acquisition system with modules NIM and VME in order to have a trigger capable to activate the acquisition only when the 4 PMTs have passed the threshold inside a window time. The setup of this system is shown in the figure 4.

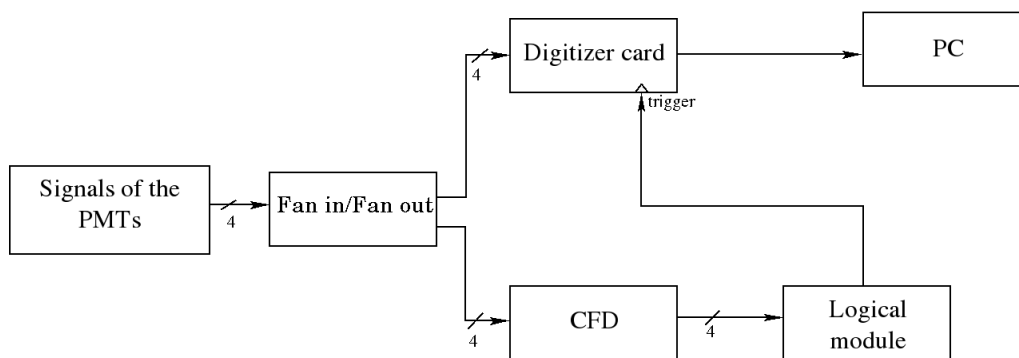


Figure 4: Block diagram for coincidence experiment.

The fan in/ fan out module mod.N625, divides the signal for digitizing and for generating the trigger signal at same time. The constant fraction discriminator module mod N842, generates a pulse with fixed width when the signal overtakes a threshold. A logical operation module mod.

V976, makes an AND operation for the four signals with pulses which assures the generation of the trigger for starting the acquisition. The resulting charge distribution of about 7 hours of data, is shown in figure 5.

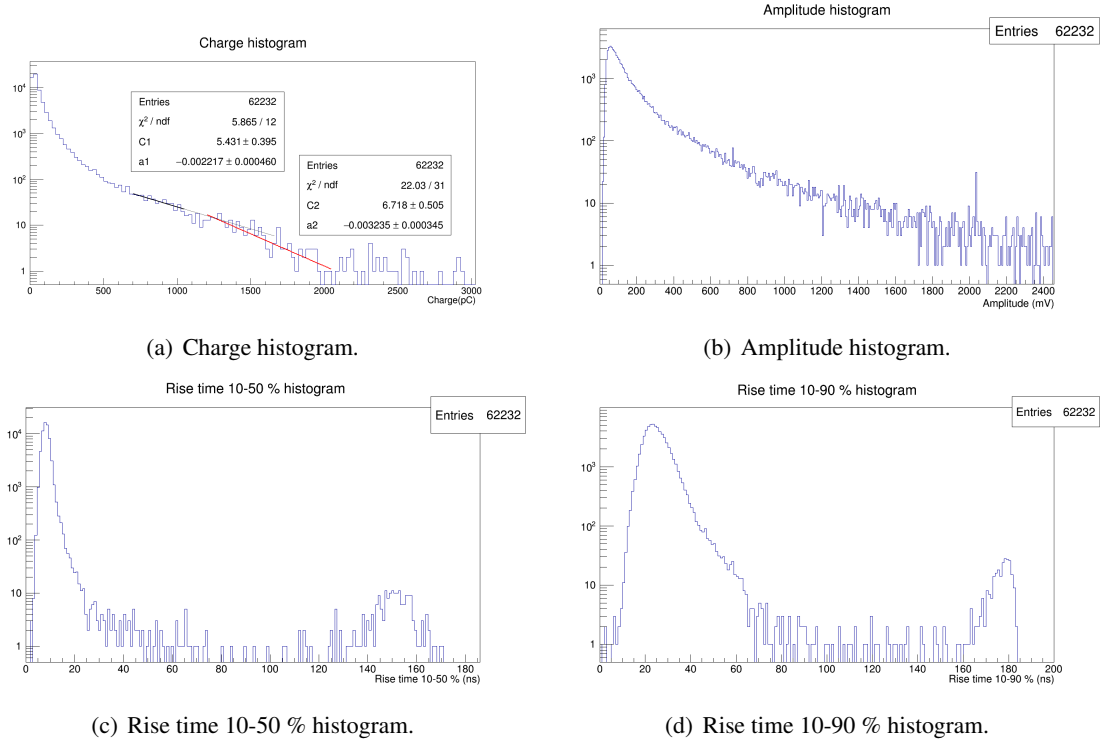


Figure 5: Calibration curves for the coincidence setup of the WCD.

A characteristic change in slope can be distinguished on the charge histogram, shown in figure 5 (a), this change can be used for calibration. The intersection of the two fitted lines of this detector can be used as a breakpoint intercalibration to the other two WCDs [6].

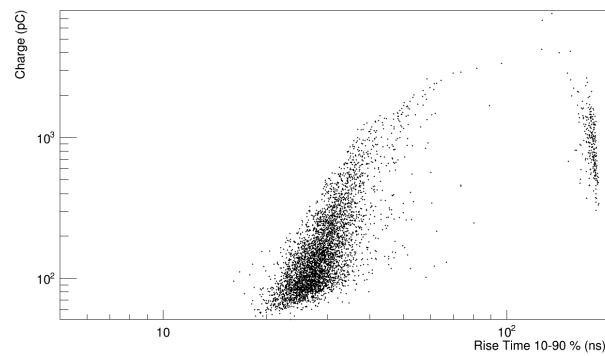


Figure 6: Correlation between charge and rise time 10-90 %, for events with amplitudes greater than 200 mV.

The bidimensional correlation plots, i.e., amplitude vs. rise time, charge vs. amplitude or charge vs. rise time as shown in figure 6, can be used to separate physical processes inside the

WCD [7] [8].

For the location of LAGO in Sierra Negra, the main contribution to the flux of secondary particles coming from cosmic rays are photons and electrons [1]. Events around 25 ns are due to electromagnetic particles. On the other hand, the measurement of the muon contents relative to the electromagnetic component give us an idea of the primary particle composition given that in heavier primary cosmic rays, the content of muons is higher [9].

4. Rate data

The acquisition rate of the first PMT started in June 2014. The installation and functionality of the entire WCD finished on January of this year. It is important to monitor the stability of the WCD. As an example we show the count rate at different threshold of one PMT. Figure 8 presents 9 day of data from February while figure 7 shows the entire month. The acquisition system is described in [10], it was implemented in rate mode and has 4 different thresholds for each PMT.

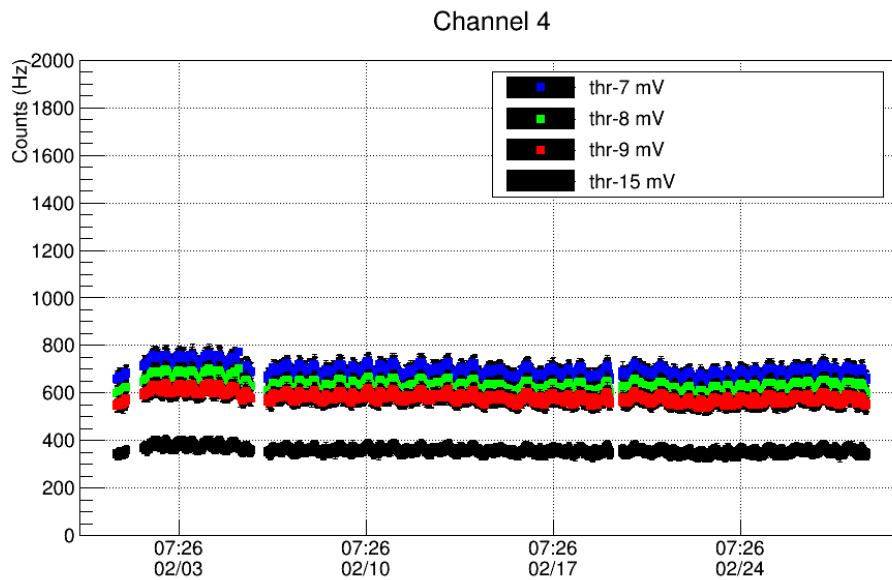


Figure 7: Data from February 2015 of the channel 4.

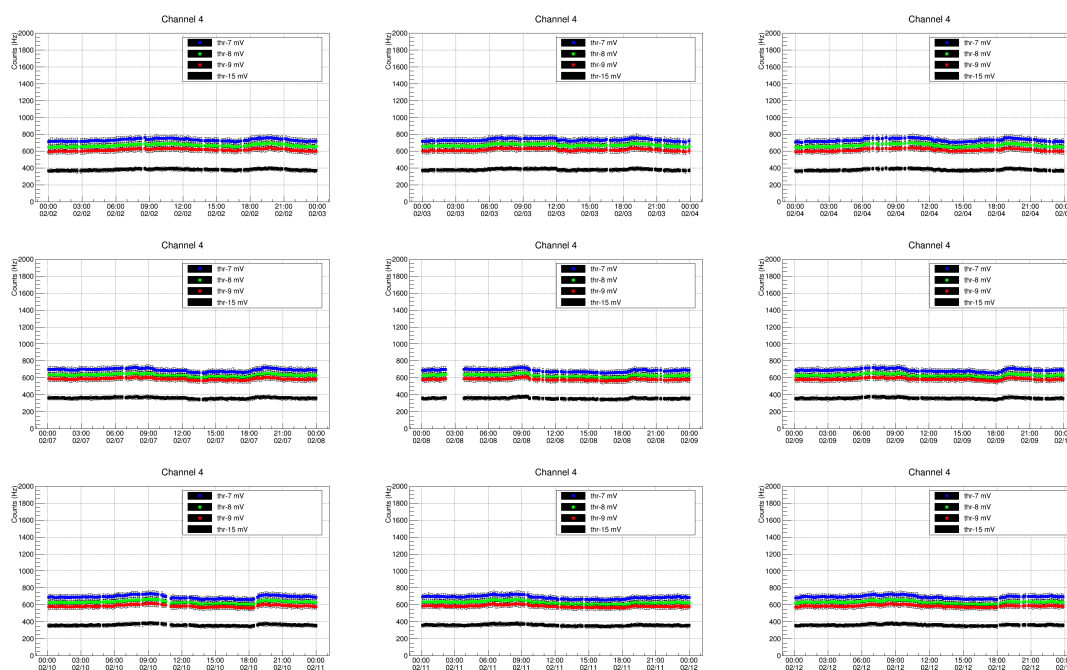


Figure 8: 9 days of data from February 2015, channel 4.

The rate mode based on single-particle rates was used as a simple estimator of the stability. The typical dispersion rms/mean was lower than 5% [7] for the analyzed data in the 4 PMTs.

5. Conclusions

An acquisition system to calibrate each PMT of the WCD has been implemented in order to obtain gain curves as a function of the voltage supply, using the SPE. After the installation of the calibrated PMTs, the characteristic curves of the WCD set in a coincidences mode were obtained and a breakpoint value of 1245 pC to fix the value for the other two WCDs. We also mentioned a method that might be useful to separate electromagnetic from muon components from the installed WCD in coincidence setup. The stability from the rate counts of the detector with less than 5% in rms/mean value were discussed from preliminary data.

References

- [1] S. Verntetto. *Astropart. Phys.* 13 (2000) 75-78.
- [2] A. K. Tripathi et al. *Nucl. Instr. and Meth. A* 497 (2003) 331-339.
- [3] D. Barnhill et al. *Nucl. Instr. and Meth. A* 591 (2008) 453-466.
- [4] E. Seo et al. *J. Korean Phys.Soc.* 35,3 (1999) 258-264.
- [5] X. Bertou et al. *Nucl. Instr. and Meth. A* 568 (2006) 839-846.
- [6] D. Allard et al. *Nucl. Instr. and Meth. A* 595 (2008) 70-72.
- [7] J. Cotzomi et al. *Nucl. Instr. and Meth. A* 553(2005) 290-294.

- [8] H. Salazar, L. Villaseñor. Nucl. Instr. and Meth. A 553 (2005) 295-298.
- [9] L. Villaseñor et al, Proc. 28th ICRC, Tsukuba (2003).
- [10] R. Conde, Proc. 33rd ICRC, Rio de Janeiro (2013).